

Cluster-variation-method simulations of the $M_{1-x}M'_xPt_3$ ($M, M' = Mn, Fe, Co$) magnetic phase diagrams with competing magnetic interactions

F. Aguilera-Granja*

Departamento de Fisica Teorica, Universidad de Valladolid, 47011 Valladolid, Spain

M. C. Cadeville, V. Pierron-Bohnes, and A. Dinia

Institut de Physique et Chimie des Matériaux de Strasbourg, Groupe d'Etude des Matériaux Métalliques UMR 46 CNRS, Université Louis Pasteur, 23 rue du Loess, F-67037 Strasbourg, France

T. H. Kim

Department of Physics, POSTECH, San 31 Hyoja-dong 790-784, Republic of Korea

(Received 6 January 1997)

The alloying of isomorphous $L1_2$ ferromagnetic $CoPt_3$, $MnPt_3$, and antiferromagnetic $FePt_3$ yields pseudobinary ($M_{1-x}M'_xPt_3$) compounds whose magnetic phase diagrams display paramagnetic, ferromagnetic, antiferromagnetic, spin glass, and reentrant spin glass regions, depending on concentration and temperature. We show that it is possible to reproduce many features of these phase diagrams, namely, the Curie and Néel temperatures, using a simple Ising Hamiltonian, treated in the pair approximation of a square cluster-variation method, with only three dominant magnetic interactions between $3d$ elements, the magnetic role of Pt being neglected. The homoatomic interactions (J_{MM} , $J_{M'M'}$) are given by the magnetic transitions of the binary compounds, whereas the heteroatomic $J_{MM'}$ interaction is either parametrized or fitted and left free to vary with concentration. [S0163-1829(97)01225-3]

The three magnetic phase diagrams of the $(Co_{1-x}Mn_x)Pt_3$, $(Co_{1-x}Fe_x)Pt_3$, and $(Mn_{1-x}Fe_x)Pt_3$ pseudobinary systems that result from alloying either two ferromagnetic $CoPt_3$ and $MnPt_3$ compounds or one ferromagnetic ($CoPt_3$ or $MnPt_3$) and one antiferromagnetic $FePt_3$ compound have been experimentally determined.¹⁻³ These phase diagrams are shown in Fig. 1. Although the binary compounds display collinear ferromagnetic (F) or antiferromagnetic (AF) structures, all the ternary systems display disordered spin states such as reentrant spin glass (RSG) or spin glass (SG) states within given temperature and concentration ranges. Typical features of these phase diagrams are (i) the occurrence of RSG phases at low temperature below the ferromagnetic phase in $(Co-Mn)Pt_3$, (ii) the occurrence of a pure spin glass phase separating the ferromagnetic side from the antiferromagnetic one in $(Co-Fe)Pt_3$ which is not observed in $(Mn-Fe)Pt_3$, and (iii) the presence of RSG phases on the ferromagnetic side in the last two systems. In terms of frustrations, the $(Co-Fe)Pt_3$ would be the most frustrated one among the three systems with the presence of a SG phase for $0.55 < x_{Fe} < 0.8$. In previous experimental reports,^{1,2} some of us have argued that the observed frustrated phases could result from a competition between pair exchange interactions with different signs. In order to see what the significant magnetic interactions are really that drive the observed magnetic phase diagrams, we present the results of a simulation model for Ising spins treated in the square approximation of a cluster-variation method using only pair correlations. This method was first developed by Mitra and Ghatak⁴ for describing magnetic phase diagrams of binary disordered systems.

We are aware of the oversimplification introduced in treating the spin systems as Ising spins but the chosen Ising

model has to be considered as a first step to treat real alloy systems with competing magnetic interactions and, as a further interest, to show also its validity limits. First the model is rapidly described. Then it is applied to the three systems in two steps. In the first step the homoatomic exchange interactions (J_{MM} , $J_{M'M'}$) are deduced from the Curie or Néel temperatures of the binary compounds and the mixed $J_{MM'}$ interactions are introduced to reproduce the transition temperatures of the ternary phases. This first step illustrates the limits of the model showing that a constant $J_{MM'}$ interaction is not able to reproduce the main features of the phase diagrams. In the second step the heteroatomic interaction is left free to change with the concentration. The obtained results illustrate the fact that $J_{MM'}$ changes its sign roughly over the concentration range where strong frustrated SG or RSG phases exist. Outside this region, where collinear F or AF orders dominate, the Curie or Néel temperatures are more or less well reproduced with a constant value of $J_{MM'}$ showing that the model works well for collinear systems, except for the $(Co-Mn)Pt_3$ system whose behavior is specific.

The model developed by Mitra and Ghatak⁴ applies to disordered magnetic binary systems with competing ferromagnetic and antiferromagnetic exchange interactions that display at low temperature unusual magnetic behaviors, marked by reentrant magnetic phase transitions, spin glass phase, etc. It was recently applied by Basu and Ghatak⁵ to ternary $(A_{1-x}B_x)_{1-r}C_r$ systems where C is a nonmagnetic element, aiming at simulating magnetic behavior of metallic glasses, in particular transition-metal-metalloid glasses. As the magnetic moment of Pt, deduced from neutron diffraction measurements, is either zero in $FePt_3$ (Ref. 6) or small compared to the $3d$ moments in $CoPt_3$ (Ref. 7) and in

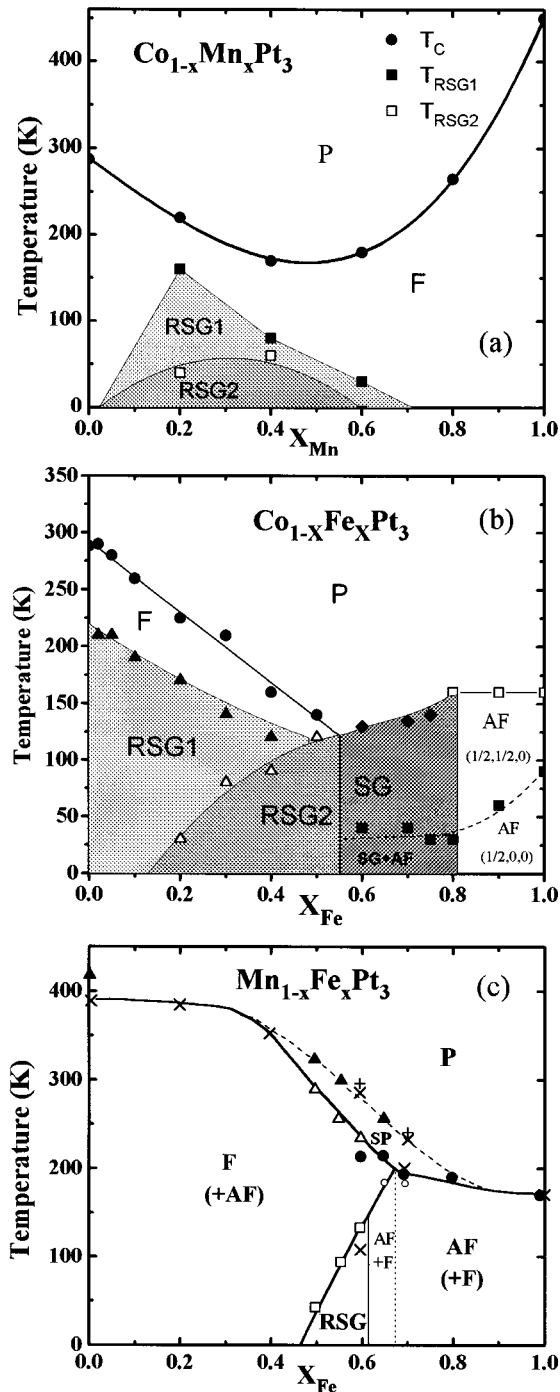


FIG. 1. Experimental magnetic phase diagrams of $(\text{Co-Mn})\text{Pt}_3$ (a), $(\text{Co-Fe})\text{Pt}_3$ (b), and $(\text{Mn-Fe})\text{Pt}_3$ (c), according to, respectively, Refs. 1–3.

MnPt_3 ,⁸ the pseudobinary systems we are interested in can be treated as the $(A_{1-x}B_x)_{1-r}C_r$ systems with $C = \text{Pt}$, and $M, M' = A$ or B and $r = 0.75$. Let us recall that the atomic structure of these compounds, when ordered, is the $L1_2$ one, where the $3d$ magnetic atoms occupy the corners of a cube and are in position of second-nearest neighbors of the fcc lattice, whereas the Pt atoms occupy the centers of the cube faces. The $3d$ atoms have 12 Pt atoms in their first shell of neighbors and 6 M or M' atoms in their second shell of neighbors. As the exchange interactions between C and A or

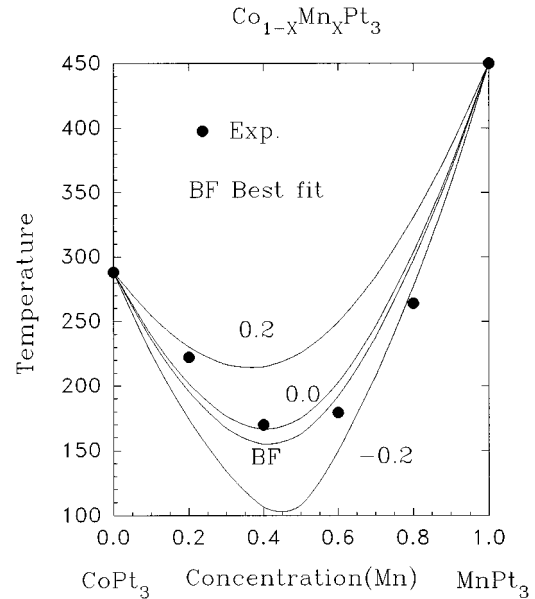


FIG. 2. Simulations of the Curie temperatures of the $(\text{Co}_{1-x}\text{Mn}_x)\text{Pt}_3$ compounds with different values of $J_{\text{Co-Mn}}$ given in the picture, compared to the experimental values (dark circles). The J values are normalized to the Curie temperature of MnPt_3 .

B atoms are taken equal to zero in Ref. 5, our problem consists of solving the case where $r = 0$, that means to treat an $M_{1-x}M'_x$ alloy disordered on a simple cubic lattice as in Ref. 4 with only three dominant magnetic exchange interactions ($J_{MM}, J_{M'M'},$ and $J_{MM'}$). Such an approximation is furthermore justified as, in these pseudoalloys, the shortest distance between $3d$ neighbors (0.35 nm) is large compared to the usual nearest neighbor distances (0.25 nm) in bcc or fcc metallic alloys. No chemical order has been observed until now between $3d$ atoms. Conversely, to treat the disordered case that we have not yet undertaken, C atoms should be considered. It is clear that any disorder between Pt and M atoms, by introducing $3d$ pairs of nearest neighbors, has drastic consequences on the magnetic properties. For example the ferromagnetism disappears in MnPt_3 ,³ whereas ferromagnetism appears in FePt_3 with disordering.⁶ Departures from stoichiometry may have similar consequences. It is the reason why the study of the magnetic properties of these ternary systems has to be strongly correlated to a thorough control of their structural state. For example, the Curie temperature of the stoichiometric MnPt_3 as thoroughly checked in Ref. 1 (450 K) is clearly higher than that given by Ref. 3 (390 K) when it corresponds to the exact stoichiometry. However, the presence of defects such as antisites or antiphase boundaries cannot be totally avoided, and one should have in mind that such defects in changing the local environments of atoms may introduce perturbations in the basic magnetic properties, giving rise in some cases to mixed F and AF phases as indicated in Figs. 1(b) and 1(c).

For example, the case of FePt_3 has been investigated in detail by neutron diffraction.⁶ The basic magnetic structure of stoichiometric and ordered FePt_3 is the $[\frac{1}{2}\frac{1}{2}0]$ AF order with a Néel temperature of 160 K. The atomic disorder and (or) the presence of APB's introduce either the $[\frac{1}{2}00]$ AF order with a Néel temperature of 80 K or ferromagnetism,

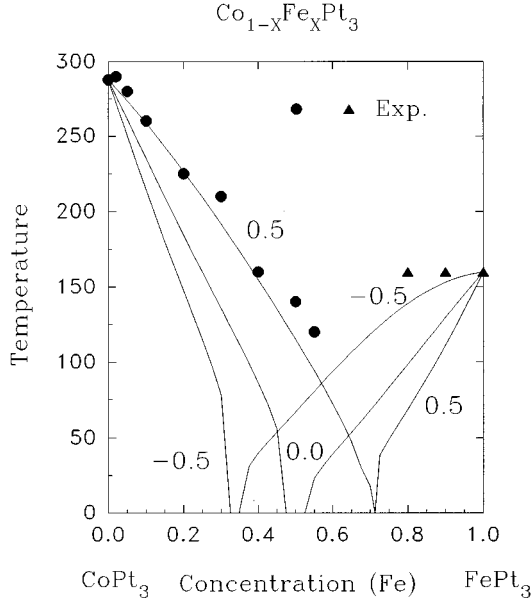


FIG. 3. Simulations of the Curie and Néel temperatures of the $(\text{Co}_{1-x}\text{Fe}_x)\text{Pt}_3$ compounds with different values of $J_{\text{Co-Fe}}$, compared to experimental values of T_C (circles) and T_N (triangles). The J values are normalized to T_C of CoPt_3 .

but all observed magnetic orders are collinear. Both AF transitions observed in $(\text{Co-Fe})\text{Pt}_3$ system are indicated on the phase diagram of Fig. 1(b). In the following simulations, we will retain only the main trends of the phase diagrams.

As described in Ref. 5, the alloy is modeled by an Ising Hamiltonian:

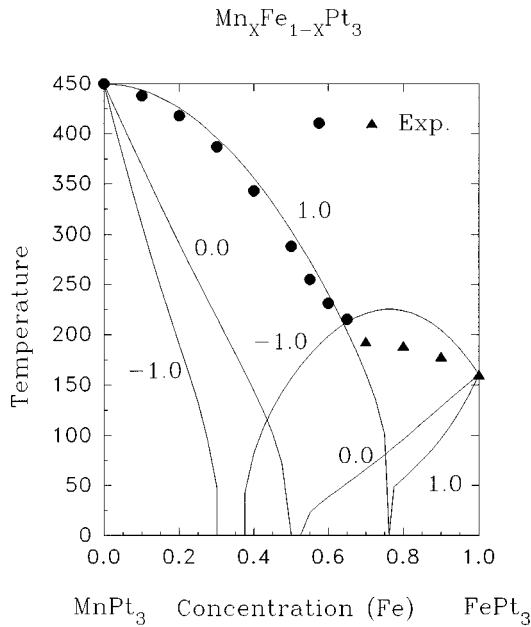


FIG. 4. As in Fig. 3 for the $(\text{Mn}_{1-x}\text{Fe}_x)\text{Pt}_3$ compounds. The J values are normalized to T_C of $\text{MnPt}_3 = 450$ K. This value, given in Ref. 1, which is slightly different from that of Ref. 3, is that which corresponds to the exact stoichiometry we have used in our simulations.

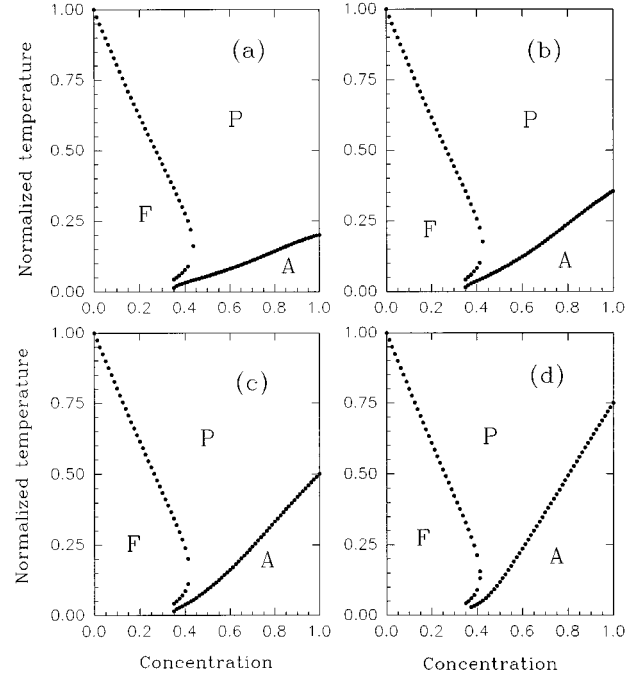


FIG. 5. Prototype phase diagrams calculated with a constant $J_{MM'}$ value of -0.1 and different negative values of the ratio $J_{M'M'}/J_{MM}$.

$$H = -\frac{1}{2} \sum_{i,j} J_{ij} S_{iz} S_{jz} - h \sum_i S_{iz}, \quad (1)$$

where the Ising spin S_{iz} at the i th site takes the value ± 1 and h is an external magnetic field. The exchange magnetic field J_{ij} takes three values J_{AA} , J_{AB} , and J_{BB} for magnetic bonds A - A , A - B , and B - B , respectively and it is zero when a C atom participates in the formation of the bond. All the exchange interactions can be ferromagnetic or antiferromagnetic in nature. The model is then treated using the cluster-variation method (CVM) developed by Kikuchi⁹ and applied by Oguchi¹⁰ to magnetic systems. This approximation in the calculation of the free energy involves the decomposition of the system into N building blocks and the use of an effective field as a variational parameter. The building blocks are taken as squares of four atoms, in which atomic bonds are exactly counted assuming a random distribution of atoms in the block. As N decreases, the free energy tends to its exact value. This approximation, called the square approximation of the pair CVM, is quite better than those most often used to calculate the free energy of Ising or Heisenberg spin systems which do not go beyond the Bragg-Williams approximation. The case treated by Basu and Ghatak in Ref. 5 was limited to ferromagnetic interactions for J_{AA} and J_{BB} and to a unique and small J_{BB}/J_{AA} ratio of 0.1 whereas phase diagrams were simulated for various J_{AB} from positive to negative, a negative value of J_{AB} being necessary to introduce frustrations, i.e., SG or RSG phases. Different situations were treated in Ref. 4 by Mitra and Ghatak.

To apply this formalism to our alloy systems, we have only to change the number of nearest neighbors (n) from 8 , the value they have arbitrarily taken, to 6 , which corresponds to the number of nearest neighbors on a simple cubic lattice.

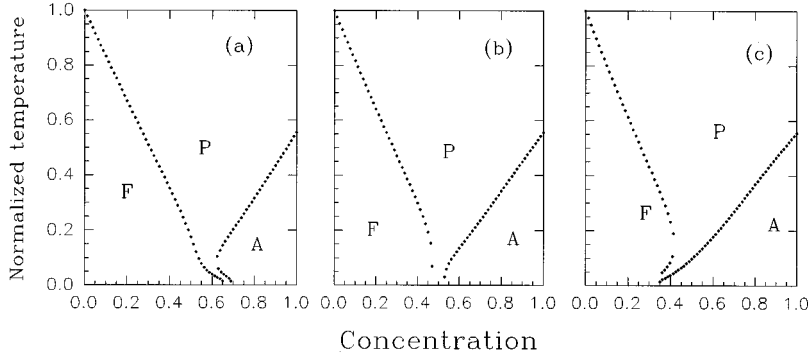


FIG. 6. Prototype phase diagrams calculated with a constant $J_{M'M'}/J_{MM}$ ratio of -0.555 [case of $(\text{Mn-Fe})\text{Pt}_3$] for three values of $J_{MM'}$ [$0.1, 0, -0.1$, respectively in (a), (b), and (c)] illustrating the great sensitivity of the phase diagram to the sign of $J_{MM'}$.

In order to see how this model works when applied to real alloy systems, we have limited our application to the calculation of the Curie and Néel temperatures whose expressions are given in Ref. 5, but not to the calculation of the spin glass transitions that is implied to calculate the zero-field susceptibility and the nonlinear susceptibility. In the simulations all the J values are normalized to the highest transition temperature of the considered system.

I. RESULTS WITH A CONSTANT $J_{MM'}$ VALUE

Results for the $(\text{Co-Mn})\text{Pt}_3$ phase diagram are shown in Fig. 2. It corresponds to the case treated in Ref. 5 with J_{CoCo} and J_{MnMn} both positive. The best fit is obtained with a small and negative value of $J_{\text{CoMn}} = -0.0437$. A negative value of J_{CoMn} is expected to introduce the frustrated bonds that originate the occurrence of reentrant spin glass phases at low temperature. Considering the curves of Fig. 2 in detail it appears that the fit is better on the Co-rich side with $J_{\text{CoMn}} = 0.2$ and on the Mn-rich side with $J_{\text{CoMn}} = -0.2$, indicating a trend for a change of J_{CoMn} with composition.

Results for the $(\text{Co-Fe})\text{Pt}_3$ and $(\text{Mn-Fe})\text{Pt}_3$ phase diagrams are shown in Figs. 3 and 4. It is clear that it is not possible to reproduce both ferromagnetic and antiferromagnetic sides of the phase diagrams with a unique value of J_{CoFe} or J_{MnFe} which would be positive on the ferromagnetic side and negative on the antiferromagnetic one.

Moreover, in order to check the influence of the coexistence of two antiferromagnetic orders in FePt_3 , yielding two different values of J_{FeFe} , we have varied J_{FeFe} over a large range including the values corresponding to the two Néel temperatures. Results are shown in Figs. 5(a)–5(d) for a value of $J_{\text{Co(Mn)Fe}} = -0.1$. It is hard to distinguish any difference between the four different diagrams calculated for $J_{\text{FeFe}} = -0.2, -0.355, -0.5, \text{ and } -0.75$, respectively. This indicates that the influence of J_{FeFe} on the concentration ranges of existence of ferromagnetic and antiferromagnetic regions is small. Conversely it is the effect of the mixed interaction which is important. This is illustrated in Fig. 6 where J_{MM} and $J_{M'M'}$ interactions are fixed to those of the $(\text{Mn-Fe})\text{Pt}_3$ system. It is clear that the stability limits of each phase and the occurrence of reentrance are strongly influenced by $J_{MM'}$. This point had been already outlined by Ref. 4. It is the reason why in the following step we limit the simulations to varying $J_{MM'}$, the value of J_{FeFe} being adjusted to the highest Néel temperature.

II. RESULTS WITH $J_{MM'}$ FREE TO CHANGE WITH CONCENTRATION

Results are collected in Figs. 7–9 where both the simulated and experimental phase diagrams are represented together with the fitted concentration dependence of $J_{MM'}$. In the $(\text{Co-Mn})\text{Pt}_3$ system, the amplitude of variation of J_{CoMn} is small but the concentration range where J_{CoMn} varies is broad. Surprisingly J_{CoMn} is positive on the Co-rich side and negative on the Mn-rich side, whereas the most frustrated side of the phase diagram is the Co-rich side: the maximum of TRSG peaks at $\text{Co}_{0.8}\text{Mn}_{0.2}\text{Pt}_3$ and no canted spin states are observed at low T on the Mn-rich side for $0.8 \leq x_{\text{Mn}} \leq 1$.¹ Although developed initially by Basu and Ghatak⁵ to describe a similar situation, it appears that, when applied to a real system, the model is too simple for the case where the frustrations are only expressed by reentrant SG phases.

In the $(\text{Co-Fe})\text{Pt}_3$ system (Fig. 8), the agreement between

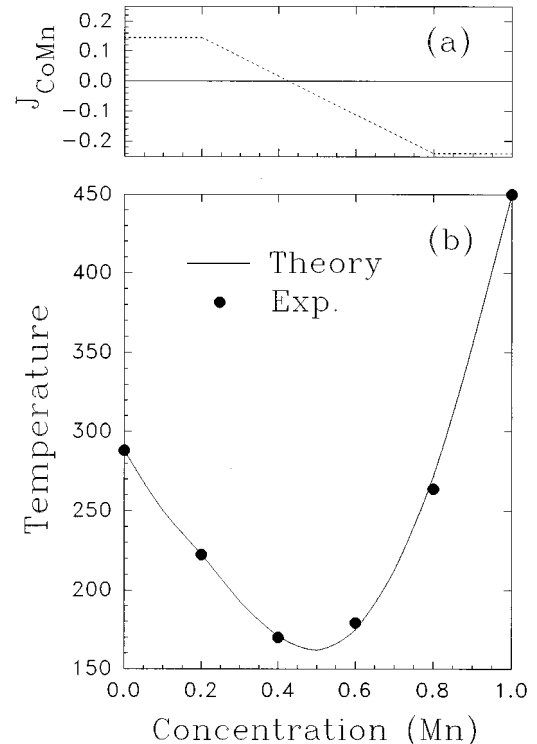


FIG. 7. Theoretical (continuous line) and experimental (circles) $(\text{Co-Mn})\text{Pt}_3$ magnetic phase diagrams and concentration dependence of J_{CoMn} corresponding to the best fit.

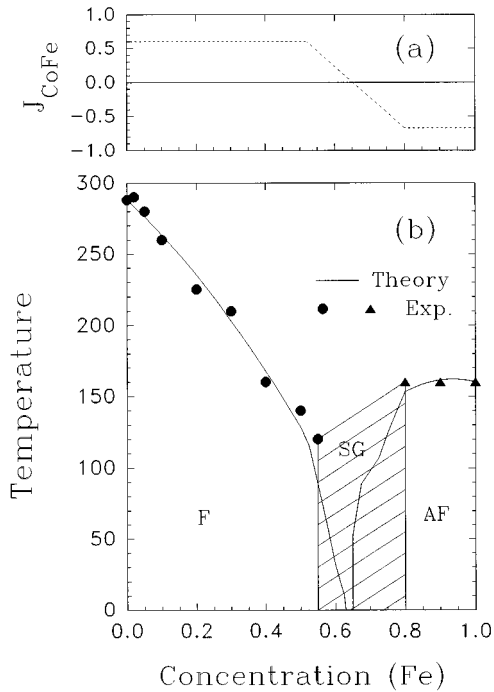


FIG. 8. The same as in Fig. 7 for (Co-Fe) Pt_3 . Experimental values are represented by circles for T_C and by triangles for T_N ; the hatched area corresponds to the spin glass region.

simulated and experimental phase diagrams is excellent on both sides of the phase diagram. The decrease of the Curie temperature is well reproduced with $J_{\text{CoFe}}=0.6$ for $0 \leq x_{\text{Fe}} \leq 0.52$ and the variation of the Néel temperature fits well with $J_{\text{CoFe}} = -0.67$ for $0.8 \leq x_{\text{Fe}} \leq 1$. The intermediate concentration range ($0.52 \leq x_{\text{Fe}} \leq 0.8$) where J_{CoFe} changes progressively from 0.6 to -0.67 corresponds roughly to the occurrence of the spin glass region where there is a strong canting of the magnetic moments. It means that when collinear orders dominate, this simple model works well with constant J_{CoCo} , J_{FeFe} , and J_{CoFe} values, but with a J_{CoFe} value which is positive on the ferromagnetic side and negative on the antiferromagnetic side. In that system the region of occurrence of the canted spin states (RSG2) does not correspond to a variation of J_{CoFe} .

Roughly the same conclusions held for the (Mn-Fe) Pt_3 system except over the narrow concentration range ($0.6 \leq x_{\text{Mn}} \leq 0.7$) where J_{MnFe} changes its sign (Fig. 9). Over that concentration range the experimental phase diagram determined by Ref. 3 displays a continuous transition line through the ferromagnetic to the antiferromagnetic region with a multicritical point for $x_{\text{Fe}}=0.67$ and $T=200$ K. No spin glass phase has been observed between the ferromagnetic region and the antiferromagnetic one, but a RSG phase is observed below the Curie temperature for $0.47 \leq x_{\text{Fe}} \leq 0.67$ indicating the presence of frustrated spin states. In most similar systems resulting from alloying ferromagnetic and antiferromagnetic phases the presence of a RSG phase below the ferromagnetic state announces the proximity of a SG phase (see, for example, Refs. 11 and 12) as it is the spin glass phase that is the reentrant phase. Due to the difficulties in getting stoichiometric and well-ordered samples, it is possible that the existence of a spin glass region, over the narrow concentration range 0.6–0.7 where

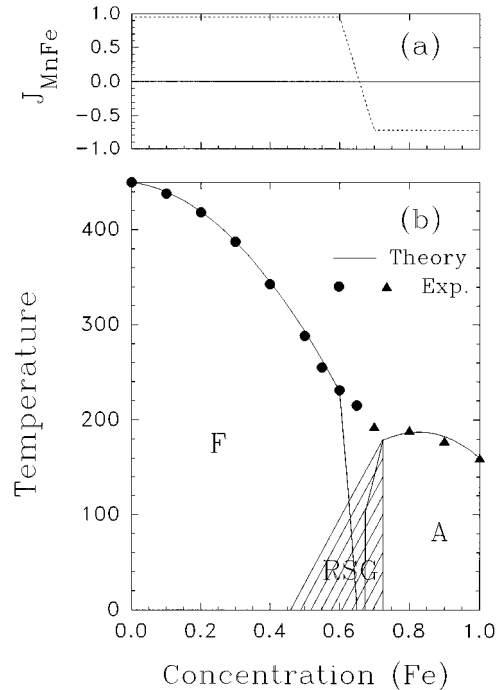


FIG. 9. The same as in Fig. 8 for (Mn-Fe) Pt_3 ; the hatched area corresponds to the RSG region.

J_{MnFe} changes its sign, has been missed by the authors of Ref. 3.

To conclude, it is clear that the Ising Hamiltonian model we use was not expected to yield a description of RSG and SG canted spin states. But it shows that, when collinear F or AF orders dominate, this model is able to reproduce the high temperature stability limits of the collinear magnetic orders, namely the Curie or Néel temperatures, with these concentration-independent exchange interactions. We believe that our simplified approach works well in these ordered $(M, M')\text{Pt}_3$ compounds because the 3d atoms have large magnetic moments and occupy a unique position (corners) of the fcc lattice, yielding predominant large direct “exchange” interactions that overcome the long-range spin-spin correlations as mediated by the electron conduction in the RKKY model.¹³ This situation is different from that usually observed in binary frustrated metallic alloys as described, for example, in Cu-Mn by Ling *et al.*¹⁴ Let us mention to conclude that a real interest in studying these $(M, M')\text{Pt}_3$ compounds with competing magnetic interactions is the possibility to explore the magnetic behavior over the whole concentration range from the ferromagnetic side to the antiferromagnetic one, by staying inside the same crystallographic structure, without significant volume change. A similar study is not possible in most of metallic binary alloys.

ACKNOWLEDGMENTS

The contribution of F.A.-G. was supported by DGICYT Grant No. SAB95-0390, CNRS-CONACYT Grant No. 164922A (France-Mexico, 1995), and CONTACYT Grant No. 961015 (Mexico).

*On leave from Instituto de Física, Universidad Autónoma de San Luis Potosí, 78000 San Luis Potosí, S. L. P., Mexico.

- ¹T. H. Kim, M. C. Cadeville, A. Dinia, and H. Rakoto, *Phys. Rev. B* **53**, 221 (1996).
- ²T. H. Kim, M. C. Cadeville, A. Dinia, V. Pierron-Bohnes, and H. Rakoto, *Phys. Rev. B* **54**, 3408 (1996).
- ³W. H. Schreiner, W. Stamm, and E. F. Wassermann, *J. Phys. F* **15**, 2009 (1985).
- ⁴A. Mitra and S. K. Ghatak, *J. Magn. Magn. Mater.* **51**, 321 (1985).
- ⁵S. Basu and S. K. Ghatak, *J. Magn. Magn. Mater.* **123**, 97 (1993).
- ⁶G. E. Bacon and J. Crangle, *Proc. R. Soc. London, Ser. A* **272**, 387 (1963).
- ⁷F. Menzinger and A. Paoletti, *Phys. Rev.* **143**, 365 (1966).
- ⁸B. Antonini, F. Lucari, F. Menzinger, and A. Paoletti, *Phys. Rev.* **187**, 611 (1965).
- ⁹R. Kikuchi, *Phys. Rev.* **81**, 988 (1951).
- ¹⁰A. Oguchi, *Prog. Theor. Phys.* **56**, 1442 (1976).
- ¹¹G. Aeppli, S. M. Shapiro, R. J. Birgeneau, and H. S. Chen, *Phys. Rev. B* **28**, 5160 (1983).
- ¹²M. Gabay and G. Toulouse, *Phys. Rev. Lett.* **47**, 201 (1981).
- ¹³M. A. Ruderman and C. Kittel, *Phys. Rev.* **96**, 99 (1954); T. Kasuya, *Prog. Theor. Phys.* **16**, 45 (1956); K. Yoshida, *Phys. Rev.* **106**, 893 (1957).
- ¹⁴M. F. Ling, J. B. Staunton, and D. D. Johnson, *Europhys. Lett.* **25**, 631 (1994).